

Synthesis, Characterization, and Reactivity of PCN Pincer Nickel Complexes

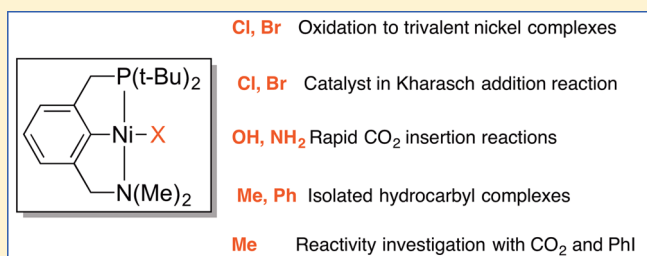
Abdelrazek H. Mousa,[†] Jesper Bendix,[‡] and Ola F. Wendt^{*,†}

[†]Centre for Analysis and Synthesis, Department of Chemistry, Lund University, P.O. Box 124, S-221 00 Lund, Sweden

[‡]Department of Chemistry, University of Copenhagen, Universitetsparken 5, DK-2100 Copenhagen, Denmark

Supporting Information

ABSTRACT: New diamagnetic nickel(II) complexes based on an unsymmetrical (1-(3-((ditert-butylphosphino)methyl)phenyl)-*N,N*-dimethyl-methanamine) (PCN) pincer ligand were synthesized and characterized by ¹H, ³¹P{¹H}, and ¹³C{¹H} NMR spectroscopy. Their molecular structures were confirmed by X-ray diffraction. Oxidation to high-valent paramagnetic Ni(III) dihalide complexes was achieved through straightforward reaction of the corresponding diamagnetic halide complexes with anhydrous CuX₂ (X = Cl, Br). In agreement with this, the complexes are active in



Kharasch addition of CCl₄ to olefins. The reaction of the hydroxo complex (8) and the amido complex (11) with CO₂ produced the hydrogen carbonate and carbamate complexes, respectively. The hydrogen carbonate complex was converted to the dinuclear nickel carbonate complex (10). The methyl (13), phenyl (14), and *p*-tolylacetylde (15) complexes are also described in the current study providing the first example of the hydrocarbyl nickel complexes based on an unsymmetric aromatic pincer ligand. Furthermore, the reactivity of the methyl complex toward different electrophiles has been investigated, showing that C–C bond formation is possible with aryl halides, whereas the reaction with CO₂ is sluggish.

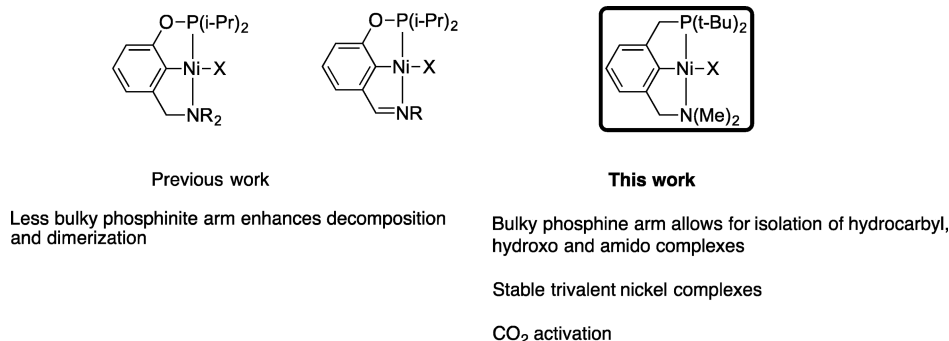
INTRODUCTION

Late transition metal complexes incorporating pincer ligand architectures have been established as an important class of organometallic compounds.^{1–12} At the early stage of development of these complexes, nickel complexes based on aromatic PCP ligands¹³ have been reported followed by NCN pincer nickel complexes^{14–18} and aliphatic PCP complexes.^{19–23} On the basis of the difference in electronic and steric properties of PCP and NCN ligands the preparation of the corresponding nickel complexes were based on different strategies: PCP nickel complexes are accessible through direct C–H activation of the corresponding PCP ligand, while lithiation of the NCN ligand is required to get the NCN nickel complexes. The differences between the two types of ligands extended further and were shown to include the outcome of both stoichiometric and catalytic reactions. For example, the use of an NCN pincer ligand enabled the isolation of high-valent nickel complexes and greatly enhanced the catalytic reactivity of their corresponding divalent nickel halide complexes in the Kharasch addition reaction of polyhalogenated hydrocarbons to olefins,^{14–18,24} while PCP pincer nickel complexes engaged in the activation of small molecules as a result of the strong coordination of the PCP ligand.^{22,23,25–27} Consequently, a variety of symmetric pincer nickel complexes have been synthesized and employed in homogeneous catalysis.^{28–39} In contrast, unsymmetric aromatic pincer nickel complexes are less represented, and the reported examples are mainly based on the unsymmetric POCN-type phosphinite amine pincer

ligand, which was extensively studied by Zargarian and more recently by Miller.^{40–44} The more electron-rich PCN pincer ligand^{45,46} with a phosphine arm is expected to undergo more facile cyclometalation with nickel compared to the POCN ligand, a hypothesis which is supported by a previous study showing that phosphine based ligands undergo faster cyclometalation of nickel compared to that of phosphinite based ones.³⁴ The presence of bulky substituents on the phosphine arm could enhance the stability of the resulting nickel complexes and help to isolate catalytically relevant intermediates, e.g., hydrocarbyl complexes, which surprisingly have not been reported with unsymmetric aromatic pincer nickel complexes. It could also influence the hemilability of the nitrogen arm. Thus, we here continue our work on unsymmetric pincer ligands^{45,46} and expand the family of unsymmetric nickel pincer complexes to include also PCN complexes, cf. Chart 1. The new complexes undergo rapid oxidation reactions to give the corresponding air and moisture stable nickel(III) complexes, and we present the first examples of hydrocarbyl, hydroxide, and amide nickel complexes with an unsymmetric aromatic pincer architecture. The reactivity of these complexes with small molecules and other electrophiles is also reported.

Received: May 18, 2018

Chart 1. This and Previous Work



EXPERIMENTAL SECTION

General Procedures and Materials. All experiments were carried out under an atmosphere of nitrogen or argon using glovebox, Schlenk, or high-vacuum-line techniques unless otherwise noted.⁴⁷ Solvents were vacuum-transferred to the reaction vessel from sodium/benzophenone ketyl radical, except for methanol, which was dried over magnesium activated with iodine and dichloromethane, obtained from an MBRAUN (MB-SPS 800) dry solvent dispenser. ¹H, ¹³C{¹H}, and ³¹P{¹H} NMR spectra were recorded on a Varian Unity INOVA 500 spectrometer operating at 499.77 MHz (¹H) or a Bruker Avance 400 FT-NMR spectrometer operating at 400.1 MHz (¹H). Chemical shifts are given in ppm downfield from TMS using residual solvent peaks (¹H and ¹³C) or H₃PO₄ (³¹P) as reference. Multiplicities are abbreviated as follows: (s) singlet, (d) doublet, (t) triplet, (q) quartet, (m) multiplet. Elemental analyses were performed by H. Kolbe Microanalytisches Laboratorium, Mülheim an der Ruhr, Germany. The *t*-butyl- and methyl-substituted PCN-H ligand ((1-(3-((di-*tert*-butylphosphino)methyl)phenyl)-*N,N*-dimethylmethanamine, henceforth called PCN-H) was synthesized following the synthetic procedures we published previously.⁴⁵

Synthesis of [PCN]Ni–Cl (1). *Method A.* DMAP (128.2 mg, 1.05 mmol) was added, in the glovebox, to a stirred mixture of the (PCN)-H ligand (308 mg, 1.05 mmol) and anhydrous NiCl₂ (203.9 mg, 1.57 mmol) in toluene (15 mL) in a Straus flask. The flask was closed, and the reaction mixture stirred for 24 h at 100 °C. After cooling to room temperature, the mixture was filtered over Celite leaving a green colored solid and the filtrate evaporated under reduced pressure giving 257 mg (63%) of complex 1 as a yellow crystalline solid.

Method B. Et₃N (0.28 mL, 2.04 mmol) was added, in the glovebox, to a stirred mixture of the (PCN)-H ligand (286 mg, 0.97 mmol) and anhydrous NiCl₂ (126 mg, 0.97 mmol) in THF (15 mL) in a Straus flask. The flask was closed, and the reaction mixture stirred for 24 h at 85 °C. After cooling to room temperature, the mixture was filtered over Celite and the filtrate evaporated under reduced pressure giving 325 mg (86.5%) of complex 1 as a yellow crystalline solid. Single crystals suitable for X-ray diffraction analysis were prepared by slow diffusion of *n*-hexane into a DCM solution of 1 at 5 °C. ¹H NMR (C₆D₆): δ = 6.99 (dd, ³J_{HH} = 7.4, 1H), 6.77 (d, ³J_{HH} = 7.4 Hz, 1H), 6.58 (d, ³J_{HH} = 7.1 Hz, 1H), 3.31 (s, 2H), 2.80 (d, ²J_{HP} = 8.7 Hz, 2H), 2.46 (s, 6H), 1.39 (d, ³J_{HP} = 12.9 Hz, 18H). ¹³C{¹H} NMR: δ = 155.4 (d, ²J_{CP} = 28.9 Hz), 149.9 (s), 149.7 (d, ³J_{CP} = 17.4 Hz), 124.9 (s), 121.7 (d, ³J_{CP} = 16.8 Hz), 119.1 (s), 72.0 (s), 48.9 (s), 34.9 (d, ¹J_{CP} = 30.7 Hz), 34.4 (d, ¹J_{CP} = 13.8 Hz), 29.5 (d, ²J_{CP} = 2.9 Hz). ³¹P{¹H} NMR: δ = 85.3 (s). Anal. Found (calcd for C₁₈H₃₁ClNPNi): C, 55.87 (55.93); H, 8.15 (8.08); N, 3.65 (3.62).

Synthesis of [PCN]Ni–Br (3). To a solution of the (PCN)-H ligand (308 mg, 1.05 mmol) in 20 mL of THF was added (DME) NiBr₂ (324.1 mg, 1.05 mmol) inside the glovebox, immediately forming an intense green color. Then, Et₃N (0.3 mL, 2.1 mmol) was added to the reaction mixture. The Straus flask was sealed, and the reaction mixture stirred for 24 h at 70 °C. After cooling to room temperature, THF and all volatiles were removed under reduced pressure and the solid dissolved in benzene, filtered over Celite, and

the solvent evaporated under reduced pressure yielding 434 mg (96%) of complex 3 as a yellowish green solid. Single crystals suitable for X-ray diffraction analysis were prepared by slow diffusion of *n*-hexane into a DCM solution of 3 at 5 °C. ¹H NMR (C₆D₆): δ = 7.00 (td, ³J_{HH} = 7.4 Hz, 1.1 Hz, 1H), 6.78 (d, ³J_{HH} = 7.5 Hz, 1H), 6.58 (d, ³J_{HH} = 7.4 Hz, 1H), 3.29 (s, 2H), 2.81 (d, ²J_{HP} = 8.9 Hz, 2H), 2.49 (d, ⁴J_{HP} = 1.4 Hz, 6H), 1.39 (d, ³J_{HP} = 13.0 Hz, 18H). ¹³C{¹H} NMR: δ = 156.9 (d, ²J_{CP} = 28.4 Hz), 149.8 (s), 149.6 (d, ³J_{CP} = 17.1 Hz), 125.1 (s), 121.6 (d, ³J_{CP} = 16.9 Hz), 119.2 (d, ⁴J_{CP} = 1.2 Hz), 71.9 (d, ³J_{CP} = 1.8 Hz), 49.6 (d, ³J_{CP} = 1.2 Hz), 35.3 (d, ¹J_{CP} = 30.7 Hz), 34.6 (d, ¹J_{CP} = 14.0 Hz), 29.7 (d, ²J_{CP} = 3.0 Hz). ³¹P{¹H} NMR: δ = 86.1 (s). Anal. Found (calcd for C₁₈H₃₁BrNPNi): C, 50.36 (50.16); H, 7.47 (7.25); N, 3.13 (3.25).

Synthesis of [PCN]Ni(III)–Cl₂ (4). To a solution of 11.6 mg (0.03 mmol) of 1 in 2 mL of DCM was added 4.0 mg (0.03 mmol) of anhydrous CuCl₂, immediately forming a red colored solution and white precipitate. The reaction was left stirring for 1 h. Filtration over Celite and evaporation of the solvent under reduced pressure yielded 11.8 mg (93%) of the product as a red solid. Single crystals suitable for X-ray diffraction analysis were prepared by slow diffusion of *n*-hexane into a DCM solution of 4 at 5 °C. Anal. Found (calcd for C₁₈H₃₁Cl₂NPNi): C, 51.10 (51.23); H, 7.16 (7.40); N, 3.12 (3.32).

Synthesis of [PCN]Ni(III)–Br₂ (5). To a solution of 12.9 mg (0.03 mmol) of 3 in 2 mL of DCM was added 6.7 mg (0.03 mmol) of anhydrous CuBr₂, immediately forming a deep brown colored solution and white precipitate. The reaction was left stirring for 1 h. Filtration over Celite and evaporation of the solvent under reduced pressure yielded 11 mg (71.8%) of the product as a fluffy violet crystalline solid. Single crystals suitable for X-ray diffraction analysis were prepared by slow diffusion of *n*-hexane into a DCM solution of 5 at 5 °C. Anal. Found (calcd for C₁₈H₃₁Br₂NPNi): C, 42.19 (42.31); H, 6.39 (6.12); N, 2.69 (2.74).

Synthesis of [PCN]Ni–ONO₂ (6). 1 (77.3 mg, 0.20 mmol) and AgNO₃ (51.0 mg, 0.30 mmol) were dissolved in 15 mL of THF. The mixture was stirred for 48 h, and the flask was protected from light by aluminum foil. After evaporation of the solvent, the residue was dissolved in benzene, filtered, and the filtrate evaporated yielding 71.9 mg (87%) of the product as an orange solid. Single crystals suitable for X-ray diffraction analysis were prepared by slow diffusion of pentane into a benzene solution of 6 at 5 °C. ¹H NMR (500 MHz, C₆D₆) δ = 6.94 (td, ³J_{HH} = 7.4, 0.9 Hz, 1H), 6.65 (d, ³J_{HH} = 7.5 Hz, 1H), 6.47 (d, ³J_{HH} = 7.3 Hz, 1H), 3.16 (s, 2H), 2.63 (d, ²J_{HP} = 8.8 Hz, 2H), 2.24 (d, ⁴J_{HP} = 1.2 Hz, 6H), 1.20 (d, ³J_{HP} = 13.2 Hz, 18H). ¹³C{¹H} NMR: δ = 150.2 (d, ³J_{CP} = 16.7 Hz), 149.7 (s), 149.5 (d, ²J_{CP} = 28.9 Hz), 125.4 (s), 122.0 (d, ³J_{CP} = 17.0 Hz), 119.7 (d, ⁴J_{CP} = 2.0 Hz), 70.3 (d, ³J_{CP} = 2.2 Hz), 47.8 (d, ³J_{CP} = 1.4 Hz), 34.0 (d, ¹J_{CP} = 13.1 Hz), 33.0 (d, ¹J_{CP} = 32.8 Hz), 28.9 (d, ²J_{CP} = 3.9 Hz). ³¹P{¹H} NMR: δ = 83.8 (s). Anal. Found (calcd for C₁₈H₃₁N₂NiO₃P): C, 52.31 (52.33); H, 7.37 (7.56); N, 6.50 (6.78).

Synthesis of [PCN]Ni–TFA (7). 1 (58 mg, 0.015 mmol) and AgTFA (35 mg, 0.016 mmol) were dissolved in 10 mL of THF. The mixture was stirred for 48 h, and the flask was protected from light by aluminum foil. After evaporation of the solvent, the residue was

dissolved in Et₂O, filtered, and the filtrate evaporated yielding 69 mg (99%) of the product as a yellow solid. Single crystals suitable for X-ray diffraction analysis were obtained from Et₂O at -20 °C. ¹H NMR (400 MHz, C₆D₆) δ = 6.94 (td, ³J_{HH} = 7.4, 1.3 Hz, 1H), 6.67 (d, ³J_{HH} = 7.5 Hz, 1H), 6.48 (d, ³J_{HH} = 7.4 Hz, 1H), 3.13 (s, 2H), 2.63 (d, ²J_{HP} = 8.9 Hz, 2H), 2.26 (d, ⁴J_{HP} = 1.5 Hz, 6H), 1.22 (d, ³J_{HP} = 13.2 Hz, 18H). ¹³C{¹H} NMR: δ = 161.7 (d, ²J_{CP} = 35.2 Hz, C=O), 150.5 (d, ³J_{CP} = 29.2 Hz), 150.0 (d, ³J_{CP} = 16.7 Hz), 149.6 (s), 125.3 (s), 121.9 (d, ³J_{CP} = 16.9 Hz), 119.5 (d, ⁴J_{CP} = 2.0 Hz), 117.1 (q, ¹J_{CF} = 291.0 Hz, CF₃), 70.6 (d, ³J_{CP} = 2.2 Hz), 48.1 (s), 33.9 (d, ¹J_{CP} = 13.1 Hz), 33.2 (d, ¹J_{CP} = 32.9 Hz), 28.9 (d, ²J_{CP} = 3.7 Hz). ³¹P{¹H} NMR: δ = 84.4(s). ¹⁹F NMR: δ = -75.0(s). Anal. Found (calcd for C₂₀H₃₁F₃NNiO₂P): C, 51.95 (51.76); H, 6.83 (6.73); N, 3.11 (3.02).

Synthesis of [PCN]Ni-OH (8). **6** (61.9 mg, 0.15 mmol) and ground KOH (168.3 mg, 3 mmol) were dissolved in 20 mL of THF. The mixture was sonicated for 5 h and then was left stirring overnight. After evaporating the solvent, the residue was dissolved in benzene, filtered inside the glovebox, and the filtrate evaporated yielding 49 mg (89%) of the product **8** as a pale yellow solid. Further reactivity indicates the presence of NaNO₃ as an impurity in **8** (see the "Results and Discussions" section for further details). ¹H NMR (500 MHz, C₆D₆) δ = 7.02 (td, ³J_{HH} = 7.4, 1.0 Hz, 1H), 6.83 (d, ³J_{HH} = 7.5 Hz, 1H), 6.66 (d, ³J_{HH} = 7.3 Hz, 1H), 3.49 (s, 2H), 2.83 (d, ²J_{HP} = 8.8 Hz, 2H), 2.61 (d, ⁴J_{HP} = 1.3 Hz, 6H), 1.29 (d, ³J_{HP} = 12.6 Hz, 18H), -2.56 (s, 1H). ¹³C{¹H} NMR: δ = 160.2 (d, ²J_{CP} = 27.8 Hz), 149.9 (d, ⁴J_{CP} = 1.9 Hz), 149.1 (d, ³J_{CP} = 17.2 Hz), 123.7 (s), 121.3 (d, ³J_{CP} = 17.1 Hz), 118.8 (d, ⁴J_{CP} = 1.7 Hz), 72.4 (d, ³J_{CP} = 1.9 Hz), 48.0 (d, ³J_{CP} = 2.0 Hz), 35.5 (d, ¹J_{CP} = 32.1 Hz), 33.7 (d, ¹J_{CP} = 12.3 Hz), 29.4 (d, ²J_{CP} = 4.0 Hz). ³¹P{¹H} NMR: δ = 84.9(s). Anal. Found (calcd for C₁₈H₃₂NNiOP): C, 59.37 (58.73); H, 8.99 (8.76); N, 3.48 (3.80).

Synthesis of [PCN]Ni-OCO₂H (9). In a J. Young NMR tube, 10 mg of (PCN)Ni-OH (**7**) was dissolved in 0.5 mL of C₆D₆ inside the glovebox. The tube was degassed (three freeze-pump-thaw cycles) on the high-vacuum line, and the solution was pressurized with 4 atm of CO₂ giving bicarbonate complex **9** and 7% nitrate complex **6**. ¹H NMR (500 MHz, C₆D₆): δ = 13.26 (bs, 1H), 6.94 (t, ³J_{HH} = 7.3 Hz, 1H), 6.69 (d, ³J_{HH} = 7.4 Hz, 1H), 6.50 (d, ³J_{HH} = 7.3 Hz, 1H), 3.24 (s, 2H), 2.69 (d, ²J_{HP} = 8.7 Hz, 2H), 2.43 (s, 6H), 1.34 (d, ³J_{HP} = 13.0 Hz, 18H). ¹³C{¹H} NMR: δ = 162.8 (s), 151.7 (d, ²J_{CP} = 29.8 Hz), 150.2 (d, ³J_{CP} = 17.2 Hz), 149.9 (s), 124.9 (s), 121.7 (d, ³J_{CP} = 16.8 Hz), 119.3 (d, ⁴J_{CP} = 1.5 Hz), 70.9 (d, ³J_{CP} = 1.9 Hz), 48.2 (s), 34.0 (d, ¹J_{CP} = 12.7 Hz), 33.4 (d, ¹J_{CP} = 32.2 Hz), 29.2 (d, ²J_{CP} = 3.8 Hz). ³¹P{¹H} NMR: δ = 82.5 (s).

Synthesis of {[PCN]Ni}(μ-CO₂) (10). Decarboxylated product **10** was obtained either by crystallization of the bicarbonate complex at -20 °C from pentane after evaporation of C₆D₆ or by decarboxylation of complex **9** on the high-vacuum line (in C₆D₆) and removing the volatiles. ¹H NMR (400 MHz, C₆D₆): δ = 7.01 (t, ³J_{HH} = 6.7 Hz, 2H), 6.78 (d, ³J_{HH} = 6.7 Hz, 2H), 6.63 (d, ³J_{HH} = 6.6 Hz, 2H), 3.44 (s, 4H), 2.93 (br. s, 12H), 2.75 (d, ²J_{HP} = 8.3 Hz, 4H), 1.47 (d, ³J_{HP} = 12.6 Hz, 36H). ¹³C{¹H} NMR: δ = 166.1 (s), 154.6 (d, ²J_{CP} = 30.7 Hz), 150.4 (d, ⁴J_{CP} = 2.7 Hz), 150.2 (s), 124.3 (s), 121.5 (d, ³J_{CP} = 16.4 Hz), 118.9 (s), 72.0 (s), 48.8 (s), 33.9 (s), 33.8 (d, ¹J_{CP} = 12.2 Hz), 29.5 (d, ²J_{CP} = 3.3 Hz). ³¹P{¹H} NMR: δ = 79.6 (s).

Synthesis of [PCN]Ni-NH₂ (11). **3** (43.1 mg, 0.1 mmol) and NaNH₂ (39.03 mg, 1 mmol) were mixed inside the glovebox in 20 mL of THF and vacuum transferred to the reaction flask. The mixture was sonicated for 5 h and then was left stirring overnight. After evaporation of the solvent, the residue was dissolved in benzene, filtered, and the filtrate evaporated giving the product as a red sticky solid in 95% yield. ¹H NMR (400 MHz, C₆D₆): δ = 7.06 (td, ³J_{HH} = 7.4, 1.3 Hz, 1H), 6.92 (d, ³J_{HH} = 7.4 Hz, 1H), 6.75 (d, ³J_{HH} = 7.3 Hz, 1H), 3.49 (s, 2H), 2.95 (d, ²J_{HP} = 8.7 Hz, 2H), 2.37 (d, ⁴J_{HP} = 1.3 Hz, 6H), 1.32 (d, ³J_{HP} = 12.4 Hz, 18H), -1.80 (s, 2H). ¹³C{¹H} NMR: δ = 165.9 (d, ²J_{CP} = 26.6 Hz), 148.42 (d, ³J_{CP} = 17.4 Hz), 148.30 (d, ⁴J_{CP} = 1.3 Hz), 123.44 (s), 121.06 (d, ²J_{CP} = 16.9 Hz), 118.70 (d, ⁴J_{CP} = 1.1 Hz), 73.33 (d, ³J_{CP} = 1.3 Hz), 48.31 (s), 37.35 (d, ¹J_{CP} = 32.1 Hz), 34.02 (d, ¹J_{CP} = 12.0 Hz), 29.63 (d, ²J_{CP} = 3.9 Hz). ³¹P{¹H} NMR: δ = 86.7 (s).

Synthesis of [PCN]Ni-OCONH₂ (12). In a J. Young NMR tube, 10 mg of **11** was dissolved in 0.5 mL of C₆D₆ inside the glovebox. The tube was degassed (three freeze-pump-thaw cycles) on the high-vacuum line, and the solution was pressurized with 4 atm of CO₂ giving the carbamate complex and an unknown side product. Complex **12** could not be isolated pure. ¹H NMR (400 MHz, C₆D₆): δ = 6.99 (td, ³J_{HH} = 7.4, 1.1 Hz, 1H), 6.74 (d, ³J_{HH} = 7.4 Hz, 1H), 6.56 (d, ³J_{HH} = 7.3 Hz, 1H), 4.00 (s, 2H), 3.32 (s, 2H), 2.73 (d, ²J_{HP} = 8.7 Hz, 2H), 2.57 (d, ⁴J_{HP} = 0.8 Hz, 6H), 1.38 (d, ³J_{HP} = 12.9 Hz, 18H). ¹³C{¹H} NMR: δ = 162.9 (s), 152.9 (d, ²J_{CP} = 30.2 Hz), 150.1 (s), 150.0 (d, ⁴J_{CP} = 2.4 Hz), 124.7 (s), 121.7 (d, ³J_{CP} = 16.7 Hz), 119.3 (s), 71.1 (s), 48.2 (s), 34.0 (d, ¹J_{CP} = 12.4 Hz), 33.7 (d, ¹J_{CP} = 32.1 Hz), 29.2 (d, ²J_{CP} = 3.8 Hz). ³¹P{¹H} NMR: δ = 81.8 (s).

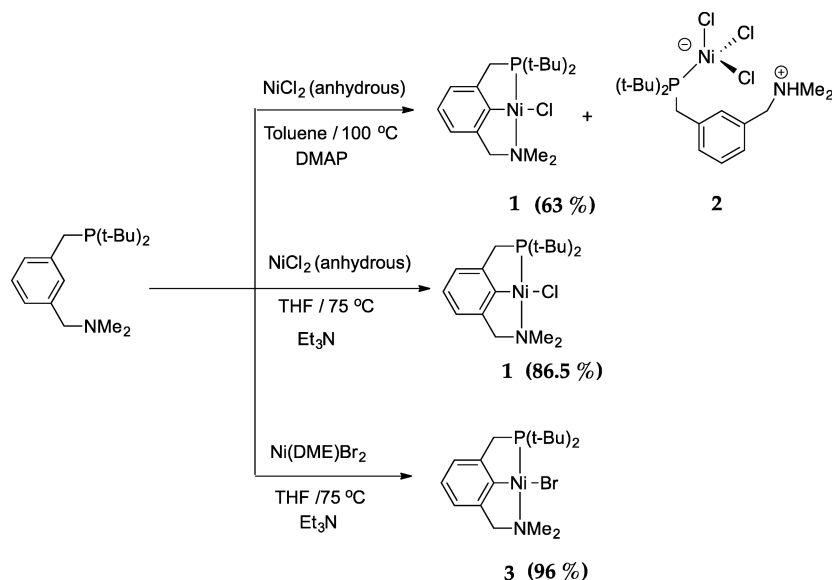
Synthesis of [PCN]Ni-Me (13). *Method A.* MeLi (40 μL of a 1.6 M solution in Et₂O, 0.064 mmol, 2 equiv) was transferred to a J. Young NMR tube inside the glovebox, and the solvent was evaporated on the high-vacuum line. The tube was introduced again to the glovebox where 0.5 mL of C₆D₆ and 12.3 mg of **1** were added. The methyl complex was formed immediately. Quenching the excess of the MeLi by water led to decomposition of the product.

Method B. A solution of 51.4 mg (0.12 mmol) of **3** in 10 mL of THF was cooled down to -78 °C, and a slight excess of MeMgCl (3 M in THF) was added dropwise. The reaction was left stirring overnight. After evaporation of the solvent, the residue was redissolved in *n*-hexane, filtered over Celite inside the glovebox, and the filtrate evaporated giving the product as a yellow solid. For further purification, the product was redissolved in *n*-hexane and washed with degassed water under a nitrogen atmosphere to remove any traces of inorganic salts. The organic layer was extracted and dried over anhydrous Na₂SO₄ followed by filtration and evaporation of the solvent. Single crystals suitable for X-ray diffraction analysis were prepared from hexane at -20 °C inside the glovebox. Yield: 39 mg (89%). ¹H NMR (500 MHz, C₆D₆): δ = 7.13 (td, ³J_{HH} = 7.3, 1.2 Hz, 1H), 7.05 (d, ³J_{HH} = 7.4 Hz, 1H), 6.86 (d, ³J_{HH} = 7.2 Hz, 1H), 3.54 (s, 2H), 3.10 (d, ²J_{HP} = 8.6 Hz, 2H), 2.26 (d, ⁴J_{HP} = 1.3 Hz, 6H), 1.28 (d, ³J_{HP} = 12.2 Hz, 18H), -0.70 (d, ³J_{HP} = 2.2 Hz, 3H). ¹³C{¹H} NMR: δ = 174.3 (d, ²J_{CP} = 22.4 Hz), 148.1 (d, ⁴J_{CP} = 1.5 Hz), 148.0 (d, ³J_{CP} = 16.9 Hz), 124.0 (s), 120.7 (d, ³J_{CP} = 16.2 Hz), 118.3 (d, ⁴J_{CP} = 1.2 Hz), 75.3 (d, ³J_{CP} = 1.2 Hz), 48.2 (d, ³J_{CP} = 1.3 Hz), 39.7 (d, ¹J_{CP} = 30.9 Hz), 34.4 (d, ¹J_{CP} = 12.9 Hz), 29.9 (d, ²J_{CP} = 3.7 Hz), -7.9 (d, ²J_{CP} = 24.2 Hz). ³¹P{¹H} NMR: δ = 90.1(s). Anal. Found (calcd for C₁₉H₃₄NPNi): C, 63.15 (62.33); H, 10.14 (9.36); N, 3.60 (3.83).

Synthesis of [PCN]Ni-Ph (14). *Method A.* In a J. Young NMR tube, 20 μL (0.04 mmol, 2.0 M in THF) of PhMgCl was added to 8.6 mg (0.02 mmol) of complex **3** in 0.5 mL of C₆D₆ inside the glovebox, and the reaction was monitored by ³¹P{¹H} NMR spectroscopy until all the starting material was consumed, giving **14** as the sole product according to the ³¹P{¹H} NMR spectra. Quenching the excess of the Grignard reagent by water led to decomposition of the product.

Method B. A solution of 43.1 mg (0.1 mmol) of **3** in 10 mL of THF was cooled down to -78 °C, and a slight excess of PhMgCl (2.0 M in THF) was added dropwise. The reaction was left stirring overnight. After evaporating the solvent, the residue was dissolved in *n*-hexane, filtered over Celite inside the glovebox, and the filtrate evaporated giving 38.5 mg (90%) of **14** as a yellow solid. Single crystals suitable for X-ray diffraction analysis were prepared from *n*-hexane at -20 °C inside the glovebox. ¹H NMR (500 MHz, C₆D₆): δ = 8.08 (d, ³J_{HH} = 6.7, 2H), 7.27 (t, ³J_{HH} = 7.4, 2H), 7.11 (m, 2H), 7.04 (d, ³J_{HH} = 7.4 Hz, 1H), 6.82 (d, ³J_{HH} = 7.2 Hz, 1H), 3.46 (s, 2H), 3.12 (d, ²J_{HP} = 8.4 Hz, 2H), 1.95 (s, 6H), 1.19 (d, ³J_{HP} = 12.5 Hz, 18H). ¹³C{¹H} NMR: δ = 174.8 (d, ²J_{CP} = 25.0 Hz), 171.9 (d, ³J_{CP} = 23.9 Hz), 149.3 (d, ⁴J_{CP} = 1.7 Hz), 148.6 (d, ³J_{CP} = 16.6 Hz), 140.3 (s), 125.9 (d, ⁴J_{CP} = 1.4 Hz), 124.6 (s), 121.9 (s), 121.0 (d, ³J_{CP} = 16.1 Hz), 118.5 (d, ⁴J_{CP} = 1.6 Hz), 75.0 (d, ³J_{CP} = 1.5 Hz), 49.2 (d, ³J_{CP} = 1.6 Hz), 39.1 (d, ¹J_{CP} = 31.4 Hz), 35.2 (d, ¹J_{CP} = 13.7 Hz), 30.1 (d, ²J_{CP} = 3.7 Hz). ³¹P{¹H} NMR δ = 88.3(s). Anal. Found (calcd for C₂₄H₃₆NPNi): C, 66.74 (67.32); H, 8.65 (8.47); N, 3.25 (3.27).

Scheme 1. Synthesis of (PCN)Ni–X



Synthesis of [PCN]Ni–*p*-tolylacetylde (15). To a mixture of 19.0 mg (0.046 mmol) of **6** and 32.0 mg (0.23 mmol) of K_2CO_3 in 5 mL of THF was added 11.7 μL (0.092 mmol) of *p*-tolylacetylene. The mixture was left stirring for 48 h at room temperature. The solvent was evaporated, the residue dissolved in *n*-hexane, filtered over Celite, and the filtrate evaporated yielding 19.0 mg (90%) of **15** as a yellow solid. Crystallization from hexane at -20 °C gave the product as yellow needles. ^1H NMR (500 MHz, C_6D_6) δ = 7.56 (d, $^3J_{\text{HH}}$ = 7.8, 2H), 7.08 (t, $^3J_{\text{HH}}$ = 7.4 Hz, 1H), 7.01 (d, $^3J_{\text{HH}}$ = 7.5 Hz, 2H), 6.95 (d, $^3J_{\text{HH}}$ = 7.5 Hz, 1H), 6.75 (d, $^3J_{\text{HH}}$ = 7.2 Hz, 1H), 3.47 (s, 2H), 3.03 (d, $^2J_{\text{HP}}$ = 8.6 Hz, 2H), 2.67 (s, 6H), 2.12 (s, 3H), 1.42 (d, $^3J_{\text{HP}}$ = 13.0 Hz, 18H). $^{13}\text{C}\{^1\text{H}\}$ NMR: δ = 168.2 (d, $^2J_{\text{CP}}$ = 26.4 Hz), 150.9 (s), 149.4 (d, $^3J_{\text{CP}}$ = 18.0 Hz), 134.0 (s), 131.0 (s), 129.10 (s), 127.6 (s), 125.0 (s), 124.1 (d, J = 30.0 Hz), 121.2 (d, $^3J_{\text{CP}}$ = 17.6 Hz), 118.8 (d, $^4J_{\text{CP}}$ = 1.7 Hz), 114.6 (d, $^4J_{\text{CP}}$ = 2.7 Hz), 73.9 (d, $^3J_{\text{CP}}$ = 1.8 Hz), 50.3 (d, $^3J_{\text{CP}}$ = 1.7 Hz), 37.5 (d, $^1J_{\text{CP}}$ = 30.1 Hz), 34.4 (d, $^1J_{\text{CP}}$ = 14.9 Hz), 29.7 (d, $^2J_{\text{CP}}$ = 3.3 Hz), 21.3 (s). $^{31}\text{P}\{^1\text{H}\}$ NMR: δ = 97.4 (s). Anal. Found (calcd for $\text{C}_{27}\text{H}_{38}\text{NNiP}$): C, 69.71 (69.55); H, 8.20 (8.21); N, 2.89 (3.00).

Reaction of [PCN]Ni–Me(13**) with CO_2 .** In a J. Young NMR tube, 10 mg of **13** was dissolved in 0.5 mL of C_6D_6 inside the glovebox. The tube was degassed (three freeze–pump–thaw cycles) on the high-vacuum line, and the solution was pressurized with 4 atm of CO_2 . The tube was heated to 100–150 °C.

Reaction of [PCN]Ni–Me(13**) with PhBr.** In a J. Young NMR tube, 10 mg of **13** was dissolved in 0.5 mL C_6D_6 inside the glovebox. The tube was degassed (three freeze–pump–thaw cycles) on the high-vacuum line and introduced to the glovebox where PhBr (2 equiv) was added. The tube was heated to 100–150 °C.

Kharasch Addition of CCl_4 to Styrene. To a mixture of CCl_4 (2.5 mL, 26 mmol) and styrene (0.80 mL, 7 mmol) in Schlenk flask were added the nickel complex (0.0227 mmol) and 3 mL of MeCN. The flask was purged with nitrogen for 15 min. The golden yellow color of the reaction mixture turned into orange or red upon stirring at room temperature overnight. The temperature was increased to 80–85 °C and the color changed to brown. The reaction was stopped after 24 h, and the reaction mixture was analyzed by GC-MS and ^1H NMR spectroscopy.

Electrochemical Measurements. Cyclic voltammetry measurements were carried out at room temperature using an Autolab PGSTAT 30 (Eco Chemie, Utrecht, The Netherlands) potentiostat equipped with GPES software and a 0.1 M solution of $(\text{Bu}_4\text{N})\text{PF}_6$ in DCM as the electrolyte. The measurements were performed in a three-electrode cell with a graphite working electrode, a Ag/AgCl reference electrode and a platinum wire as an auxiliary electrode using

1 mM concentration of the halide complexes (**1** or **3**). The solutions were purged with nitrogen before conducting the experiments.

Magnetic Susceptibility and Magnetization. The magnetic data were acquired on a Quantum-Design MPMS-XL SQUID magnetometer. Susceptibility data were acquired in a static field of 2.0 kOe. Magnetization data were obtained with selected fields from 0 to 50 kOe at 2 K. The polycrystalline samples were measured on a compacted powder sample. The diamagnetic contribution to the sample moment from the sample holder and sample was corrected through background measurements and Pascal constants, respectively.

EPR Spectroscopy. The EPR spectra were recorded with a Bruker Elexsys E500 equipped with a Bruker ER 4116 DM dual-mode cavity, an EIP 538B frequency counter, an ER035 M NMR Gauss meter, and an Oxford Instruments iTC cryocontroller. The spectra were recorded at X-band frequencies ($\nu \approx 9.63$ GHz). The spectra were simulated using lab-written software considering an electronic spin of 1/2 and taking into account only the experimentally resolvable interactions with the nuclear spins of one bromide ($I = 3/2$) and one phosphorus ligand ($I = 1/2$). No distinction was made between the naturally occurring bromine isotopes. Simulation parameters are given in the legends pertinent to the individual spectra.

Crystallography. Intensity data were collected with an Oxford Diffraction Excalibur 3 system, using ω -scans and Mo $K\alpha$ ($\lambda = 0.71073$ Å) radiation.⁴⁸ The data were extracted and integrated using Crystalis RED.⁴⁹ The structures were solved by direct methods and refined by full-matrix least-squares calculations on F^2 using SHELXT,⁵⁰ SHELXL,⁵¹ and OLEX^{2,52}. Molecular graphics were generated using Crystal Maker 8.7.⁵³

RESULTS AND DISCUSSIONS

Synthesis of (PCN)Ni Complexes with Halide Ligands.

Cyclometalation of the PCN ligand⁴⁵ with anhydrous NiCl_2 in toluene in the presence of 4-dimethylaminopyridine (DMAP) at 100 °C led to formation of complex **1** as a yellow solid in 63% yield as shown in Scheme 1. We previously used a similar procedure to prepare aliphatic pincer nickel halide complexes.^{21,22} The $^{31}\text{P}\{^1\text{H}\}$ NMR spectrum of the product showed a singlet peak at $\delta = 85.3$ ppm and the ^1H NMR spectrum is divided into two regions where the aliphatic region includes the *tert*-butyl protons as a doublet, the NMe_2 protons as a singlet, the CH_2P protons as a doublet, and the CH_2N ones as a singlet, and the aromatic region contains three protons reflecting the tridentate chelation of the PCN ligand

the nickel center. The moderate yield is due to formation of a paramagnetic byproduct (**2**), which was completely NMR-silent. Attempts to isolate **2** in pure form were not successful. However, single crystals suitable for X-ray diffraction were obtained after many attempts giving the molecular structure of **2** as shown in Figure 1. The nickel center has a tetrahedral

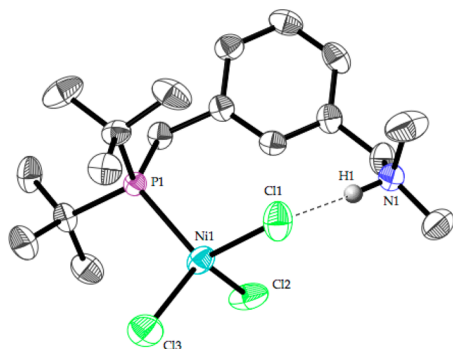


Figure 1. Molecular structure of complex **2** at the 50% probability level. Hydrogen atoms (except on N1) are omitted for clarity. Selected bond lengths (Å) and bond angles (deg): Ni1–Cl1 = 2.2865(8), Ni1–Cl2 = 2.2629(7), Ni1–Cl3 = 2.2500(7), Ni1–P1 = 2.3764(6), Cl1–Ni1–Cl2 = 102.65(3), Cl1–Ni1–Cl3 = 116.56(3), Cl2–Ni1–Cl3 = 110.99(3), Cl1–Ni1–P1 = 110.28(3), Cl2–Ni1–P1 = 108.12(2), Cl3–Ni1–P1 = 107.94(2).

geometry where it coordinates three chloride ligands and the remaining coordination site is occupied by the protonated PCN ligand through the phosphorus side arm in a monodentate fashion. Such byproducts have been observed or suggested in the cyclometalation of both aliphatic and aromatic pincer ligands with nickel precursors, but no molecular structure has been reported.^{19,21,22,40} The low yield of complex **1** induced us to further optimize the reaction conditions by (i) using 1:1 stoichiometry of the PCN ligand and the nickel precursor (NiCl₂), (ii) using THF as a solvent to enhance the solubility of the nickel precursor, and (iii) replacing the weak aromatic DMAP base with the stronger aliphatic Et₃N base to avoid the protonation of the amine arm of the PCN ligand. Indeed, the new reaction conditions helped to improve the yield, and **1** was obtained in 86% yield without formation of **2**. When (DME)NiBr₂ was used as a nickel precursor instead of anhydrous NiCl₂ following the modified

synthetic procedures of Campora for (^{i-Pr}PCP)Ni–Br,⁵⁴ (PCN)Ni–Br (**3**) was obtained in 96% yield as a yellowish green solid. Its spectroscopic features are similar to those of **1**. The higher yield achieved in the latter case could be attributed to the higher solubility and/or reactivity of molecular (DME)NiBr₂ compared to the inorganic salt NiCl₂.

To the best of our knowledge, complexes **1** and **3** are the first nickel complexes based on an unsymmetric PCN pincer ligand with a phosphine arm. Examples of nickel complexes based on the electron-deficient POCN analogue are known in the literature.^{40–44}

The molecular structures of the new halide complexes **1** and **3** are shown in Figure 2 together with selected bond distances and angles. The square planar coordination geometry around the nickel is slightly distorted.

The N1–Ni1–P1 angle in **3** (164.96(5)) is slightly larger than that in (^{i-Pr}POCN^{Me})Ni–Br (163.81(6)),⁴⁰ which we attribute to the presence of the oxygen atom in the latter pushing the phosphinite arm toward the aromatic ring. Furthermore, the Ni–Br bond length in **3** is slightly longer than that in (^{i-Pr}POCN^{Me})Ni–Br (2.3818(3) vs 2.3407(5)) indicating the expected stronger trans influence of the PCN system in comparison to the more electron deficient POCN system.

Cyclic voltammetry measurements of complexes **1** and **3** in DCM (Figure 3) showed irreversible oxidation peaks at $E_{1/2}$ = 0.837 and 0.797 V for **1** and **3**, respectively. These values of the oxidation potentials are lower than the corresponding values for POCN nickel complexes (ca. 1.0 V), which is in line with the expected, higher donicity of the PCN ligand. Thus, the high valent PCN nickel(III) complexes could be readily available through oxidation of the corresponding PCN nickel(II) complexes.

Indeed, reaction of complexes **1** and **3** with anhydrous CuX₂ salts (X = Cl, Br) in DCM produced the corresponding Ni(III) complex (Scheme 2). Within seconds after the addition of the oxidizing agent at room temperature, the yellow solution of the halide complexes turned a deep red or violet color with precipitation of white CuX salts. ¹H and ³¹P{¹H} NMR spectra of the isolated products displayed no signal due to their paramagnetic nature.

The molecular structures of complexes **4** and **5** were confirmed by X-ray diffraction measurements and the molecular structures are given in Figure 4. Both of the

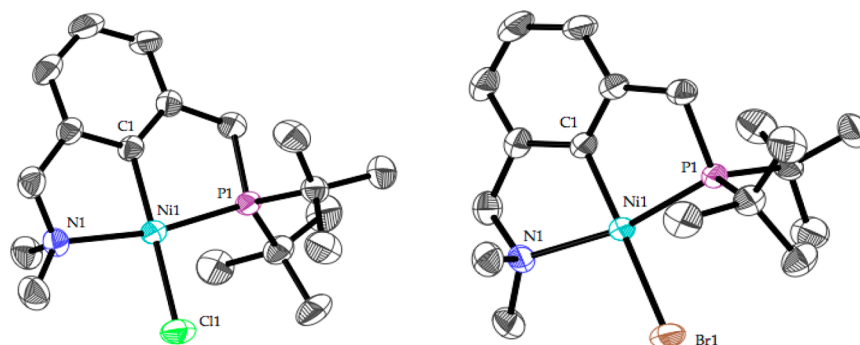


Figure 2. Molecular structures of complex **1** and **3** at the 50% probability level. Hydrogen atoms are omitted for clarity. Selected bond lengths (Å) and bond angles (deg): For complex **1** Ni1–Cl1 = 1.881(3), Ni1–P1 = 2.1643(9), Ni1–N1 = 2.028(3), Ni1–Cl1 = 2.2329(9), Cl1–Ni1–Cl1 = 177.41(10), Cl1–Ni1–P1 = 83.98(10), Cl1–Ni1–N1 = 83.66(12), N1–Ni1–P1 = 164.87(8), P1–Ni1–Cl1 = 98.04(4), N1–Ni1–Cl1 = 94.58(8). For complex (**3**) Ni1–Cl1 = 1.8921(18), Ni1–P1 = 2.1826(5), Ni1–N1 = 2.0435(16), Ni1–Br1 = 2.3818(3), Cl1–Ni1–Br1 = 177.06(6), Cl1–Ni1–P1 = 83.83(6), Cl1–Ni1–N1 = 83.71(7), N1–Ni1–P1 = 164.96(5), P1–Ni1–Br1 = 98.278(16), N1–Ni1–Br1 = 94.48(5).

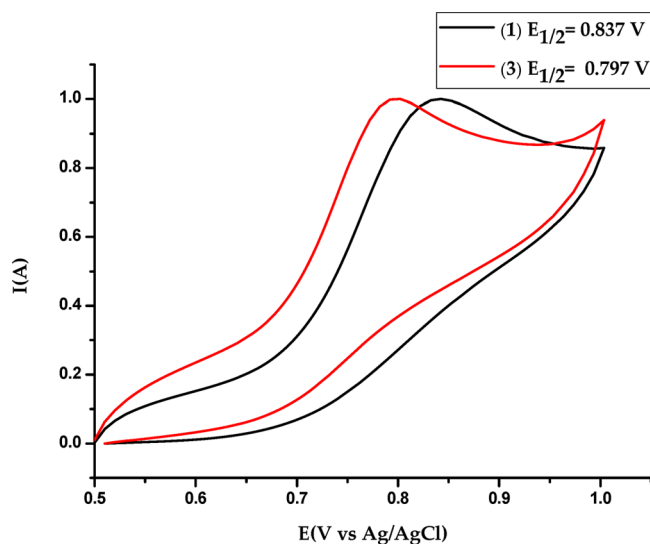
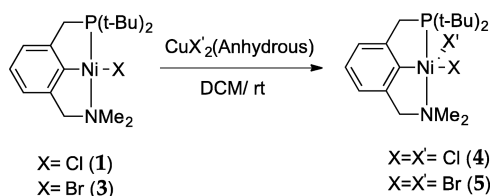


Figure 3. Cyclic voltammogram of 1 mM solutions of complexes 1 and 3 in DCM containing 0.1 M $(\text{Bu}_4\text{N})\text{PF}_6$ at a scan rate of 0.1 V/s on a glassy carbon working electrode.

Scheme 2. Synthesis of $(\text{PCN})\text{Ni}-\text{X}_2$



complexes display distorted square pyramidal coordination geometries around nickel with a halide in the apical position. The distinct elongation in the Ni–halide bond lengths (0.04 and 0.06 Å for 4 and 5, respectively) along the apical direction indicates an electronic structure with the unpaired electron located in the d_{z^2} orbital directed along Ni1–Cl1 and Ni1–Br1, respectively, as corroborated by EPR spectroscopy (*vide infra*).

Magnetic Susceptibility and Magnetization. To probe the paramagnetic properties and the electronic structure of

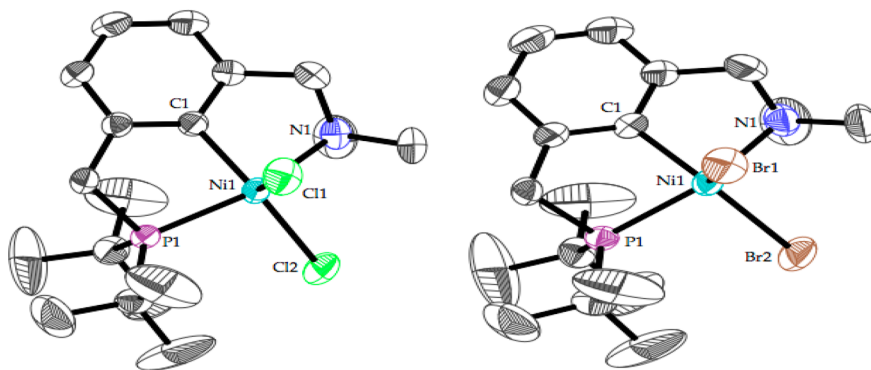


Figure 4. Molecular structures of complexes 4 and 5 at the 50% probability level. Hydrogen atoms are omitted for clarity. Selected bond lengths (Å) and bond angles (deg): For complex (4) Ni1–C1 = 1.928(3), Ni1–P1 = 2.2667(8), Ni1–N1 = 2.072(2), Ni1–Cl1 = 2.2888(8), Ni1–Cl2 = 2.2496(9), C1–Ni1–Cl1 = 90.41(8), C1–Ni1–Cl2 = 163.41(8), C1–Ni1–P1 = 81.79(8), C1–Ni1–N1 = 84.06(11), N1–Ni1–P1 = 156.57(8), P1–Ni1–Cl1 = 103.43(3), P1–Ni1–Cl2 = 95.10(3). For complex (5) Ni1–C1 = 1.928(5), Ni1–P1 = 2.2802(15), Ni1–N1 = 2.079(5), Ni1–Br1 = 2.4430(9), Ni1–Br2 = 2.3818(9), C1–Ni1–Br1 = 89.66(16), C1–Ni1–Br2 = 165.49(16), C1–Ni1–P1 = 82.09(17), C1–Ni1–N1 = 84.0(2), N1–Ni1–P1 = 155.76(15), P1–Ni1–Br1 = 104.71(5), P1–Ni1–Br2 = 94.97(5).

these complexes, complex 5 was subjected to a magnetic susceptibility and magnetization measurement and EPR analysis. The oxidation and spin-state is unequivocally demonstrated by the magnetic data, with the χT product behaving as expected for a low-spin d^7 system with $g_{\text{average}} > 2.00$ (cf. Figure 5). The expected value for a perfectly isolated

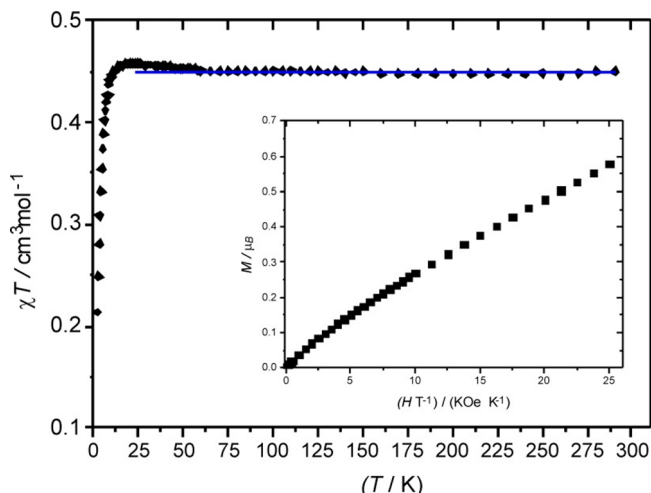


Figure 5. Magnetic susceptibility, represented by the χT product in the temperature range 2–300 K for complex 5. The inset shows magnetization data for the same sample recorded at 2 K.

system with $g_{\text{average}} = 2.19$ is $0.450 \text{ cm}^3 \text{ mol}^{-1}$, and this is shown as the blue line in Figure 5. There is a small but distinct upturn in the χT value at around 30–10 K followed by a steep decrease at the lowest temperatures. This could indicate a weak ferromagnetic interaction in pairs; indeed, there is a weak nonclassical hydrogen bond between the apical bromide and the meta C–H group on an adjacent phenyl ring, (cf. Figure S26). It is overtaken by an overall antiferromagnetic order below ca. 5 K. The magnetization is close to linear in field and does not reach saturation even at 2 K.

EPR Spectroscopy. An EPR spectrum of complex 5 was recorded on an undiluted solid sample at 11 K (cf. Figure S24). The featureless spectrum can be well-represented as an axial $S = 1/2$ spectrum with $g_{\perp} = 2.206 > g_{\parallel} = 2.065$ ($g_{\text{average}} = 2.159$).

At room temperature, a CH_2Cl_2 solution furnishes an isotropic spectrum ($g_{\text{iso}} = 2.172$) with a resolvable hyperfine structure ($A_{\text{iso}} = 0.0053 \text{ cm}^{-1}$), stemming from strong coupling to one $I = 3/2$ nucleus (cf. Figure S25). As >98% of the naturally occurring Ni isotopes have $I = 0$, this coupling must be a hyperfine coupling from the unpaired electron in the d_{z^2} orbital to a single bromide ligand corroborating a solution structure similar to the solid-state structure. A further resolved spectrum is obtained in a frozen glass ($\text{CH}_2\text{Cl}_2/\text{toluene}$; 2:1, $T = 20\text{K}$) as shown in Figure 6. In this spectrum, the extreme anisotropy

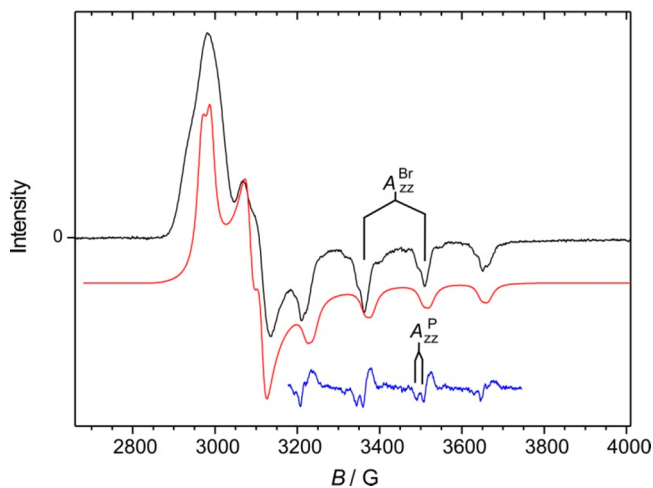


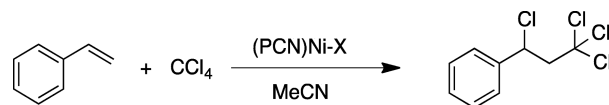
Figure 6. Experimental (black) and simulated (red) X-band EPR spectra of **5** in a frozen $\text{CH}_2\text{Cl}_2/\text{toluene}$ (2:1) glass at $T = 20\text{ K}$. The blue curve is the derivative of the experimental spectrum indicating superhyperfine splitting also from coupling to one phosphorus nucleus. The spectrum was recorded with $P = 6.325 \text{ mW}$; modulation amplitude = 3.0 G ; modulation freq = 100 kHz . Simulation parameters: $g_1 = 2.301$; $g_2 = 2.208$; $g_3 = 2.000$, $A_{zz}^{\text{Br}} = 0.0132 \text{ cm}^{-1}$, $A_{zz}^{\text{P}} = 0.0015 \text{ cm}^{-1}$, Lorentzian derivative line shape, fwhh = 15.5 G .

of the hyperfine coupling to the bromide ligand is evident with a completely dominating $A_{zz} = 0.0132 \text{ cm}^{-1}$, amounting to almost three times the A_{iso} determined from the isotropic solution spectrum at RT. Strongly anisotropic hyperfine coupling in low-spin nickel(III) systems with $A_{zz} \gg A_{\text{iso}}$ is in accordance with previous observations on e.g. heteroleptic cyano complexes and Jahn–Teller distorted homoleptic systems.^{55,56} Furthermore, a weak coupling to the phosphine ligand ($I = 1/2$) can be resolved in the parallel direction yielding $A_{zz}^{\text{P}} = 0.0015 \text{ cm}^{-1}$. The simulated frozen solution spectrum requires, in accordance with the solid-state structure, a nonaxial g -tensor ($g_1 = 2.301$; $g_2 = 2.208$; $g_3 = 2.000$) in order to achieve a satisfactory reproduction of the experimental spectrum.

Catalytic Activity in Kharasch Addition Reaction. The aromatic NCN nickel pincer complexes developed by van Koten are known to be efficient catalysts for Kharasch addition reaction of polyhalogenated alkanes to olefins.^{16,17,24} In contrast, the aromatic PCP nickel pincer analogues are not suitable as catalysts in this reaction mainly because they do not produce the corresponding trivalent nickel complexes, which are considered to be important intermediates in the catalytic cycle of the Kharasch addition reaction.¹⁷ The Kharasch addition is synthetically important because it generates a new C–C bond and introduces functionality in two positions. The facile preparation and successful isolation of the PCN

nickel(III) complexes in addition to their stability in the solid state for a long time at room temperature points toward their potential application as catalyst in Kharasch addition reaction (Scheme 3). Thus, the addition of CCl_4 to styrene in

Scheme 3. Kharasch Addition of CCl_4 to Styrene Using **1** and **3** as Catalyst



DCM at room temperature was screened using complex **1** as a catalyst under reaction conditions the same as those reported by van Koten. There was no reaction at room temperature as seen by GC-MS and ^1H NMR spectroscopy, but a change in the color from yellow to red was observed upon stirring the reaction mixture overnight probably due to the oxidation of the nickel complex to its corresponding trivalent state. Changing the solvent to acetonitrile had no effect at room temperature, but heating the reaction mixture to $80\text{--}85\text{ }^\circ\text{C}$ for 24 h led to a change in the color from orange to brown. Analyzing the reaction mixture by GC-MS and ^1H NMR spectroscopy confirmed the formation of the expected 1:1 anti-Markovnikov Kharasch addition product (100% selectivity). Bromo complex **3** was more efficient giving 95% conversion based on the ^1H NMR spectroscopy compared to 87% conversion using **1** (Table 1). A similar difference in the catalytic activity between

Table 1. Catalytic Kharasch addition reaction of CCl_4 to styrene using PCN nickel complexes **1** and **3**

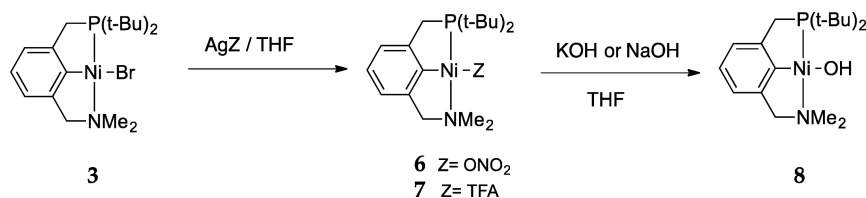
| entry | catalyst | cat. loading (%) | T ($^\circ\text{C}$) | t (h) | conversion (%) | selectivity (%) |
|-------|----------|------------------|--------------------------|---------|----------------|-----------------|
| 1 | 1 | 0.32 | 25 | 24 | 0 | |
| 2 | 3 | 0.32 | 25 | 24 | 0 | |
| 3 | 1 | 0.32 | 80–85 | 24 | 87 | 100 |
| 4 | 3 | 0.32 | 80–85 | 24 | 95 | 100 |

halide complexes has been observed earlier with NCN nickel complexes¹⁷ and is in agreement with the oxidation potentials which show that **3** is more easily oxidized. The catalyst loading in the current study is 0.32%, six times smaller than that reported for the POCN nickel pincer complex which gave a similar result.⁴⁰ This result allows an estimation of the catalytic efficiency of nickel pincer complexes in the Kharasch addition reaction and the following order appears: $\text{NCN} > \text{POC}_{\text{sp}}\text{OP} > \text{PCN} > \text{POCN}$.⁴⁰

Synthesis and Reactivity of Hydroxo and Amido Complexes. In general, hydroxo and amido nickel pincer complexes are not common in the literature compared to the corresponding halide complexes, and the reported examples only involve PCP pincer ligands.^{23,25,27,57,58} Thus, we were interested in preparing these complexes and study their reactivity toward small molecules to investigate the influence of the weak amine arm in these transformations.

Synthesis of (PCN)Ni–OH and Its Reaction with CO_2 . The hydroxo complex (**8**) was synthesized through two synthetic steps as shown in Scheme 4 following the procedures reported by Campora and us.^{23,25,46,59,60} The OH proton appears as a singlet peak at -2.56 ppm in the ^1H NMR spectrum. Although an excess of silver nitrate was used to prepare complex **6**, no further oxidation to Ni(III) complex

Scheme 4. Synthesis of (PCN)Ni–OH, 8



was observed as reported in the case of (NCN)Ni–ONO₂ and (*i*-PrPCP)Ni–ONO₂.^{14,54} Complex 8 is also accessible through reaction of complex 7 with NaOH in THF.

Unfortunately, attempts to grow crystals of complex 8 were not successful, but a single crystal of 6 was obtained by slow diffusion of *n*-hexane into a concentrated benzene solution of 6 at 5 °C. The molecular structure of complex 6 is shown in Figure 7.

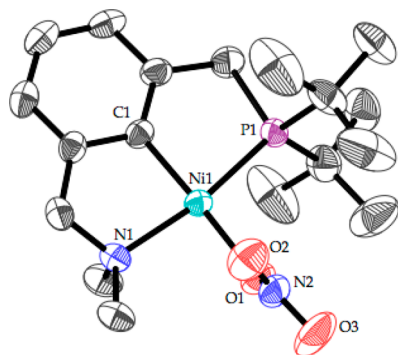
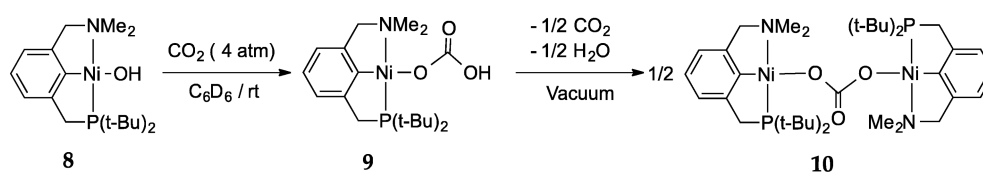


Figure 7. Molecular structure of 6 at the 50% probability level. Hydrogen atoms are omitted for clarity. Selected bond lengths (Å) and bond angles (deg): Ni1–C1 = 1.8782(13), Ni1–P1 = 2.1863(7), Ni1–N1 = 2.0242(19), Ni1–O1 = 1.9762(18), O1–N2 = 1.308(3), O2–N2 = 1.226(3), O3–N2 = 1.240(3), C1–Ni1–P1 = 84.19(5), N1–Ni1–P1 = 164.42(6), O1–Ni1–P1 = 97.46(6), O1–Ni1–N1 = 93.60(8), C1–Ni1–O1 = 177.17(8).

Reaction of 8 with 4 atm of CO₂ produced, within minutes at room temperature, a new pincer complex, 9, as seen from the ³¹P{¹H} and ¹H NMR spectra (cf. Scheme 5). The ¹H NMR spectrum of 9 features a broad singlet at 13.26 ppm which was assigned as an acidic hydrogen carbonate proton. The hydrogen carbonate group –OCO₂H was also observed as a singlet at 162.8 ppm in the ¹³C{¹H} NMR spectrum, and complex 9 was unambiguously assigned as the hydrogen carbonate complex. Complex 8 was fully consumed, and in addition to 9 a small amount of 6 was seen in the ³¹P NMR spectrum. Complex 6 is not visible in the ³¹P NMR spectrum of 8, and this indicates that there is small amount of nitrate source present in 8 and that this readily displaces the hydrogen carbonate once 9 is formed. Free CO₂ was also observed in the ¹³C{¹H} NMR spectrum at 124.8 ppm as a sharp singlet.⁶¹

Scheme 5. Reaction of CO₂ with 8

This observation suggests that the carboxylation reaction could be carried out at lower pressures. Complex 9 was also prepared in situ with 96% purity based on ³¹P NMR spectroscopy using another batch of the hydroxo complex (originally prepared by the reaction of (PCN)Ni–TFA and NaOH and which was contaminated by 4% of the (PCN)Ni–TFA complex). Removing the volatiles from complex shows that the CO₂ insertion is reversible, and in line with this, crystallization of 9 gave the dimeric carbonate complex, 10 (cf. Scheme 5). Similar results were previously reported for the palladium analog but in that case the decarboxylation required heating under vacuum.⁴⁶ Under CO₂ pressure there is no tendency for 9 to interconvert to 10. The low steric hindrance imposed by the presence of smaller substituents on the nitrogen donor atom apparently favors the dimerization. Complex 10 gave X-ray quality crystals, and the molecular structure of the dimeric complex is displayed in Figure 8.

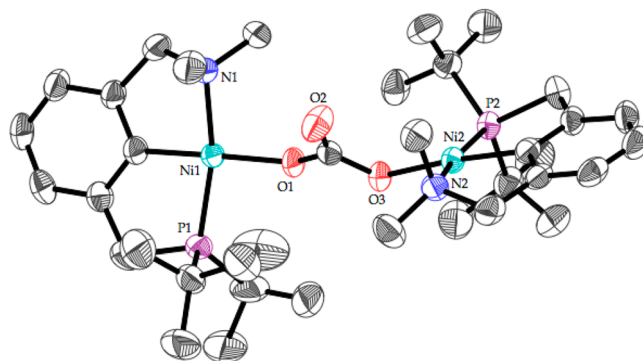
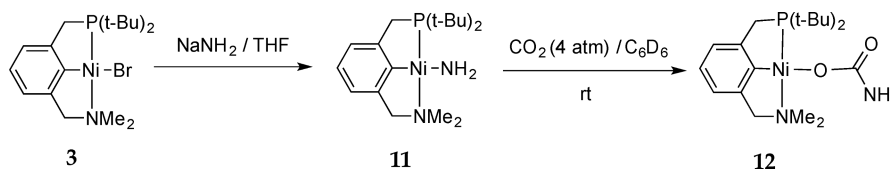


Figure 8. Molecular structure of 10 at the 50% probability level. Selected bond lengths (Å) and bond angles (deg): Ni1–P1 = 2.1518(10), Ni1–N1 = 2.014(3), Ni1–O1 = 1.902(2), Ni2–P2 = 2.1470(10), Ni2–N2 = 2.008(3), Ni2–O2 = 1.901(2), O1–Ni1–P1 = 94.25(8), O1–Ni1–N1 = 97.69(11), N1–Ni1–P1 = 168.02(9), O2–Ni2–P2 = 94.04(8), O2–Ni2–N2 = 98.37(11), N2–Ni2–P2 = 165.17(9).

Synthesis of (PCN)Ni–NH₂ and Its Reaction with CO₂.

Amido complex 11 was obtained directly from 3 as described in Scheme 6 through a salt metathesis reaction with NaNH₂ following literature procedures.⁵⁸ The complex is extremely air- and moisture-sensitive. It produces 8 in contact with trace amounts of water; this can be used as an alternative method for

Scheme 6. Insertion of CO₂ into Ni–NH₂ Bond of 11

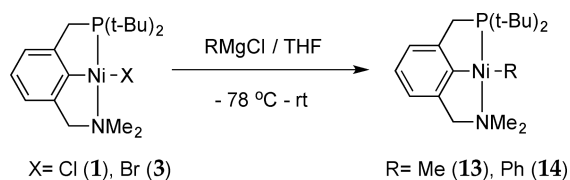
preparing hydroxide complexes as previously reported for (*t*-Bu₂PCP)Ni–OH.²⁷ The amido protons appear as a singlet in the ¹H NMR spectrum at –1.80 ppm.

The reaction of 11 with 4 atm of CO₂ in C₆D₆ was monitored by ³¹P{¹H}- and ¹H NMR spectroscopy and showed the immediate consumption of 11 and the formation of two products in a 93:7 ratio based on ³¹P NMR spectrum. The major product shows a downfield singlet peak at 3.49 ppm in the ¹H NMR spectrum assigned to the two protons of a carbamate group, and the complex was assigned as the carbamate complex, 12. The carbamate group –COONH₂ appeared as a sharp singlet peak at 162.9 ppm in the ¹³C{¹H} spectrum. Attempts to identify the minor product were unsuccessful.

Synthesis of (PCN)Ni Hydrocarbyl Complexes.

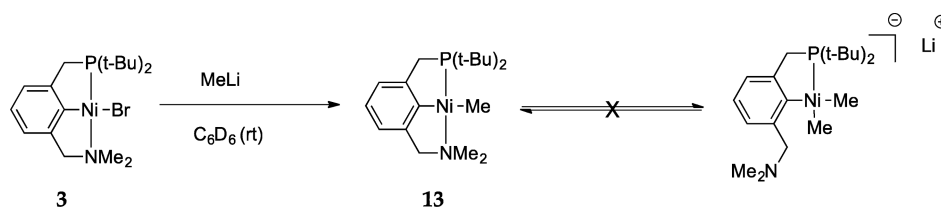
Although a few examples of unsymmetric aromatic pincer nickel halide complexes have been published, the corresponding hydrocarbyl complexes have not been reported yet. Therefore, we were interested in preparing such complexes particularly to investigate their reactivity toward electrophiles.^{22,26} Previous attempts from Zargarian and co-workers to react a POCN nickel chloride complex with a secondary amine arm with MeLi did not give the corresponding methyl complex.⁴¹ In contrast to this, a small scale reaction of 1 with MeLi immediately and cleanly produced the methyl complex 13 based on NMR spectroscopy (cf. Scheme 7). The methyl

Scheme 7. Synthesis of (PCN)Ni–R



protons appeared at –0.7 ppm as a doublet with ³J_{HP} = 2.2 Hz in the ¹H NMR spectrum. No other complexes were formed, indicating that the nickel methyl complex is inert toward further substitution reactions as reported for the palladium methyl complex based on the same ligand framework, which underwent subsequent reaction with MeLi to displace the nitrogen arm and form the dimethyl complex.⁴⁵ This indicates that the hemilability of the (PCN)Ni system is lower than that of the corresponding palladium complexes (Scheme 8).

Scheme 8. Reaction of (PCN)Ni–Br Complex with an Excess of MeLi



Attempts to isolate the methyl complex using aqueous workup was not successful, and instead, complex 3 was reacted with MeMgCl in THF at –78 °C producing 13, which was successfully extracted by *n*-hexane to remove excess of the Grignard reagents and the *in situ* formed salt. The phenyl complex 14 was obtained in an analogous way.

These hydrocarbyl complexes are stable in air in the solid state at room temperature for several days. Their molecular structures (Figures 9 and 10) were corroborated using X-ray

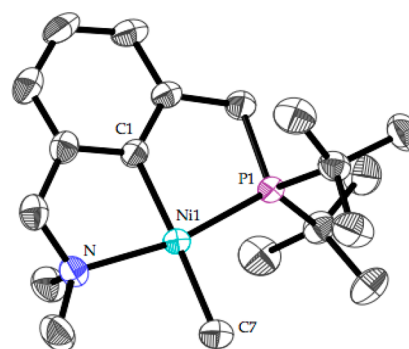


Figure 9. Molecular structure of 13 at the 50% probability level. Hydrogen atoms are omitted for clarity. Selected bond lengths (Å) and bond angles (deg): Ni1–C1 = 1.902(2), Ni1–P1 = 2.1302(6), Ni1–N1 = 2.0391(17), Ni1–C7 = 1.983(2), C1–Ni1–C7 = 175.64(9), C1–Ni1–P1 = 83.77(6), C1–Ni1–N1 = 82.96(8), N1–Ni1–P1 = 164.57(5), C7–Ni1–P1 = 99.63(7), C7–Ni1–N1 = 94.03(9).

diffraction. Both complexes have the expected square-planar structures, and the phenyl ligand is approximately perpendicular to the coordination plane in 14. Complex 13 has a slightly shorter Ni–Me bond distance than (*t*-Bu₂PCP)Ni–Me and (*t*-Bu₂POCyOP)Ni–Me complexes: 1.983(2) Å vs 2.026(2) and 2.016(3).^{22,26}

Reaction of 3 with EtMgCl in C₆D₆ did not produce the expected ethyl complex, and, instead, a characteristic signal for ethylene was observed in the ¹H NMR spectrum at 5.25 ppm⁶¹ strongly suggesting a β -hydride elimination pathway. However, no hydride complex was observed, and the free PCN ligand was formed based on NMR spectroscopy, which could be attributed to further decomposition where the *in situ* generated hydride complex undergoes reductive elimination. Similarly, bromide complex 3 reacts with hydride sources, e.g., LiAlH₄,

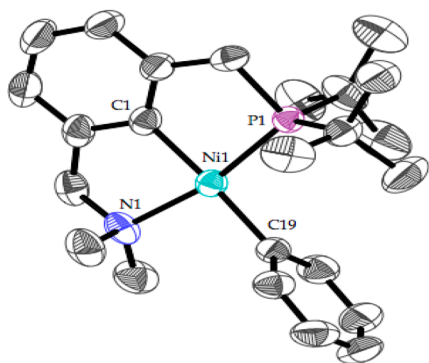
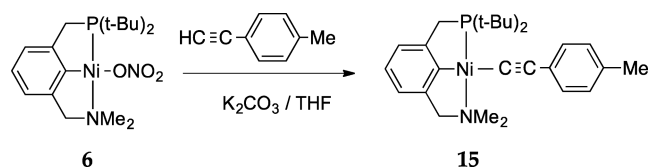


Figure 10. Molecular structures of **14** at the 50% probability level. Hydrogen atoms are omitted for clarity. Selected bond lengths (Å) and bond angles (deg): Ni1–C1 = 1.915(5), Ni1–P1 = 2.1583(14), Ni1–N1 = 2.047(4), Ni1–C19 = 1.950(5), C1–Ni1–C19 = 176.3(2), C1–Ni1–P1 = 83.05(17), C1–Ni1–N1 = 83.6(2), N1–Ni1–P1 = 166.62(15), C19–Ni1–P1 = 100.08(15), C19–Ni1–N1 = 93.3(2).

NaBH_4 , and KH , not giving the expected hydride complex but rather the free PCN ligand together with a black precipitate. Using stronger hydride sources, e.g., LiEt_3BH and Ph_2SiH_2 , gave the same result, and an immediate change in the color from yellow to brown after addition of the hydride source was observed in all the reactions. Decomposition to the free ligand was observed previously in an attempt to prepare $(^c\text{-HexPCP})\text{-Ni-H}$ by reaction of the corresponding chloride complex with LiAlH_4 .⁶² Furthermore, Hu found that the complex $(^{\text{Me}}\text{N}_2\text{N})\text{-Ni-H}$ decomposed through two routes including intramolecular reductive elimination to form the ligand.⁶³ The facile decomposition of the ethyl and the hydride complexes with the current PCN framework could be explained by the small steric hindrance of the nitrogen side arm of the PCN ligand, which could speed up the decomposition. Using more bulky substituents in the nitrogen donor atom could solve this problem and make these complexes more accessible.

The acetylide complex, **15**, is expected to be more stable than the methyl and phenyl complexes and was obtained through the straightforward synthetic method shown in Scheme 9; the same method was previously used for the

Scheme 9. Synthesis of $(\text{PCN}^{\text{Me}})\text{Ni-p-tolyl}$ acetylide



corresponding palladium complex and the use of base is crucial.⁴⁶ The identity of **15** was confirmed using X-ray crystallography, and the molecular structure is given in Figure 11.

Reactivity of the Methyl Complex toward Electrophiles. The reaction of the methyl complex with PhBr in C_6D_6 was studied (Scheme 10). The reaction was carried out in a J. Young NMR tube and monitored by $^{31}\text{P}\{^1\text{H}\}$ and ^1H NMR spectroscopy. There was no reaction at room temperature, and increasing the temperature to 50°C gave the same result. However, reaction took place at 120°C based on the $^{31}\text{P}\{^1\text{H}\}$ NMR spectra, giving **3** and the cross coupling product,

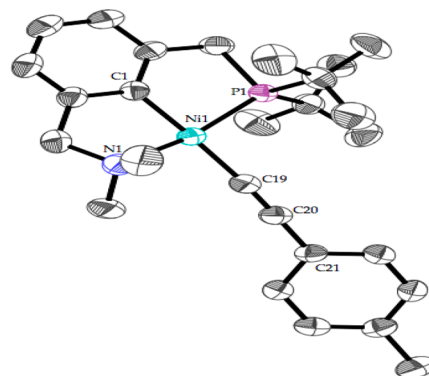


Figure 11. Molecular structure of **15** at the 50% probability level. Hydrogen atoms are omitted for clarity. Selected bond lengths (Å) and bond angles (deg): Ni1–C1 = 1.902(3), Ni1–P1 = 2.1535(8), Ni1–N1 = 2.035(3), Ni1–C19 = 1.908(3), C20–C19 = 1.218(4), C21–C20 = 1.452(4), C1–Ni1–C19 = 176.60(12), C1–Ni1–P1 = 84.28(9), C1–Ni1–N1 = 84.10(11), N1–Ni1–P1 = 163.29(8), C19–Ni1–P1 = 97.37(9), C19–Ni1–N1 = 94.88(11), C19–C20–C21 = 178.1(3).

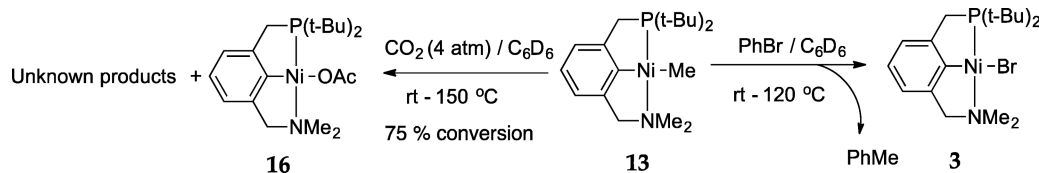
toluene, which was observed in the ^1H NMR spectrum after 24 h. 88% conversion of the starting complex was calculated based on the $^{31}\text{P}\{^1\text{H}\}$ NMR spectroscopy after 3 days.

Carboxylation of the methyl complex using 4 atm of CO_2 was monitored by NMR spectroscopy. A mixture of different products was formed at 120°C , and due to the slow progress of the reaction, the temperature was increased to 150°C and the reaction monitored over 6 days at this temperature. At that point, a small amount of black precipitate had formed prompting discontinuation of the reaction. Only the remaining methyl complex and the expected carboxylated product, the acetate complex, **16**, were identified from the mixture of the formed compounds. The acetate complex, **16**, was prepared independently from the reaction of the corresponding chloride and silver acetate. The electron deficiency of our system together with the potential decoordination of the amine arm at high temperature could explain the competing decomposition. However, the carboxylation of the more electron-rich aliphatic and aromatic PCP pincer nickel complexes did not achieve full conversion to the carboxylated product and in both cases other unknown products were observed probably due to the harsh condition.^{22,26} Overall, the current results corroborate the sluggish reactivity of the Ni–C bond toward CO_2 .

CONCLUSIONS

New nickel(II) complexes based on the unsymmetric PCN pincer ligand were synthesized and characterized. As previously reported for similar compounds, the synthesis is hampered by the formation of a tetrahedral Ni(II) complex, and this was characterized for the first time by X-ray diffraction. High-valent paramagnetic Ni(III) complexes were successfully isolated, and the Ni(III)(Br)_2 system was characterized by magnetic measurements and EPR spectroscopy, giving insight into the electronic structure of the Ni(III) complexes. The PCN framework gives a more electron-rich metal center compared to that with previously reported POCN ligands, and this gives a higher reactivity in the Kharasch addition. The reactivity of the halide complexes toward Grignard reagents allowed the isolation of the corresponding methyl and phenyl complexes that represent the first example of alkyl and aryl nickel complexes based on an unsymmetric aromatic pincer ligand.

Scheme 10. Reactivity of Complex 13 with Electrophiles



Reaction of the nickel-methyl bond with CO₂ is sluggish as previously reported for similar nickel complexes, but the reaction with aryl bromide is straightforward giving the C–C coupling product.

■ ASSOCIATED CONTENT

📄 Supporting Information

The Supporting Information is available free of charge on the ACS Publications website at DOI: [10.1021/acs.organomet.8b00333](https://doi.org/10.1021/acs.organomet.8b00333).

Selected NMR spectra, solid state and RT solution X-band EPR spectra of **5**, and crystallographic tables for complexes **1–6**, **10**, and **13–15** (PDF)

Accession Codes

CCDC [1842118–1842127](https://www.ccdc.cam.ac.uk/data_request/cif) contain the supplementary crystallographic data for this paper. These data can be obtained free of charge via www.ccdc.cam.ac.uk/data_request/cif, or by emailing data_request@ccdc.cam.ac.uk, or by contacting The Cambridge Crystallographic Data Centre, 12 Union Road, Cambridge CB2 1EZ, UK; fax: +44 1223 336033.

■ AUTHOR INFORMATION

Corresponding Author

*E-mail: ola.wendt@chem.lu.se

ORCID

Jesper Bendix: [0000-0003-1255-2868](https://orcid.org/0000-0003-1255-2868)

Ola F. Wendt: [0000-0003-2267-5781](https://orcid.org/0000-0003-2267-5781)

Notes

The authors declare no competing financial interest.

■ ACKNOWLEDGMENTS

Financial support from the Swedish Research Council, the Knut and Alice Wallenberg Foundation and the Royal Physiographic Society in Lund is gratefully acknowledged. We would like to thank Galina Pankratova for assistance in the electrochemical measurements.

■ REFERENCES

- Albrecht, M.; van Koten, G. Platinum Group Organometallics Based on “Pincer” Complexes: Sensors, Switches, and Catalysts. *Angew. Chem., Int. Ed.* **2001**, *40*, 3750–3781.
- Singleton, J. T. The uses of pincer complexes in organic synthesis. *Tetrahedron* **2003**, *59*, 1837–1857.
- van der Boom, M. E.; Milstein, D. Cyclometalated Phosphine-Based Pincer Complexes: Mechanistic Insight in Catalysis, Coordination, and Bond Activation. *Chem. Rev.* **2003**, *103*, 1759–1792.
- Morales-Morales, D.; Jensen, C. M., Eds. *The Chemistry of Pincer Compounds*; Elsevier Science B.V.: Amsterdam, 2007.
- Selander, N.; Szabó, K. J. Catalysis by Palladium Pincer Complexes. *Chem. Rev.* **2011**, *111*, 2048–2076.
- van Koten, G. Organometallic pincer chemistry. *Top. Organomet. Chem.* **2013**, *40*, 1.
- Szabó, K. J.; Wendt, O. F., Eds. *Pincer and Pincer-Type Complexes*; Wiley-VCH Verlag GmbH & Co. KGaA, 2014.
- Asay, M.; Morales-Morales, D. Non-symmetric pincer ligands: complexes and applications in catalysis. *Dalton Trans.* **2015**, *44*, 17432–17447.
- van Koten, G.; Gossage, R. A., Eds. *The Privileged Pincer-Metal Platform: Coordination Chemistry & Applications*; Springer International Publishing, 2016.
- Murugesan, S.; Kirchner, K. Non-precious metal complexes with an anionic PCP pincer architecture. *Dalton Trans.* **2016**, *45*, 416–439.
- Morales-Morales, D., Ed. *Pincer Compounds. Chemistry and Applications*; Elsevier: Amsterdam, 2018.
- Valdés, H.; García-Eleno, M. A.; Canseco-Gonzalez, D.; Morales-Morales, D. Recent Advances in Catalysis with Transition-Metal Pincer Compounds. *ChemCatChem* **2018**, *10*, 1–38.
- Moulton, C. J.; Shaw, B. L. Transition metal-carbon bonds. Part XLII. Complexes of nickel, palladium, platinum, rhodium and iridium with the tridentate ligand 2,6-bis[(di-*t*-butylphosphino)methyl]phenyl. *J. Chem. Soc., Dalton Trans.* **1976**, 1020–1024.
- Grove, D. M.; van Koten, G.; Zoet, R.; Murrall, N. W.; Welch, A. J. Unique stable organometallic nickel(III) complexes; syntheses and the molecular structure of [Ni{C₆H₃(CH₂NMe₂)₂-*o,o'*}]₂. *J. Am. Chem. Soc.* **1983**, *105*, 1379–1380.
- Grove, D. M.; van Koten, G.; Ubbels, H. J. C.; Zoet, R.; Spek, A. L. Organonickel(II) complexes of the tridentate monoanionic ligand *o,o'*-bis[(dimethylamino)methylphenyl] (N-C-N). Syntheses and the x-ray crystal structure of the stable nickel(II) formate [Ni(N-C-N)O₂CH]. *Organometallics* **1984**, *3*, 1003–1009.
- Grove, D. M.; van Koten, G.; Verschuuren, A. H. M. New Homogeneous Catalysts in the Addition of Polyhalogenoalkanes to Olefins; Organonickel(II) Complexes [Ni{C₆H₃(CH₂NMe₂)₂-*o,o'*}X] (X = Cl, Br, I). *J. Mol. Catal.* **1988**, *45*, 169–174.
- Grove, D. M.; Verschuuren, A. H. M.; van Koten, G.; van Beek, J. A. M. The homogeneously catalysed addition reaction of polyhalogenoalkanes to olefins by divalent arylnickel complexes: comparative reactivity and some important mechanistic leads. *J. Organomet. Chem.* **1989**, *372*, C1–C6.
- Van Beek, J. A. M.; van Koten, G.; Ramp, M. J.; Coenjaarts, N. C.; Grove, D. M.; Goubitz, K.; Zoutberg, M. C.; Stam, C. H.; Smeets, W. J. J.; Spek, A. L. Influence of the amino substituents of potentially bis ortho chelating aryl ligands (2,6-{R¹R²NCH₂})₂C₆H₃)[−] on the synthesis and properties of their organonickel(II) complexes. *Inorg. Chem.* **1991**, *30*, 3059–3068.
- Castonguay, A.; Sui-Seng, C.; Zargarian, D.; Beauchamp, A. L. Syntheses and Reactivities of New PC_{sp}₃P Pincer Complexes of Nickel. *Organometallics* **2006**, *25*, 602–608.
- Castonguay, A.; Beauchamp, A. L.; Zargarian, D. Preparation and Reactivities of PCP-Type Pincer Complexes of Nickel. Impact of Different Ligand Skeletons and Phosphine Substituents. *Organometallics* **2008**, *27*, 5723–5732.
- Jonasson, K. J.; Wendt, O. F. Synthesis and characterisation of new PC_{sp}₃P-supported nickel complexes. *J. Organomet. Chem.* **2014**, *759*, 15–18.
- Jonasson, K. J.; Wendt, O. F. Synthesis and Characterization of a Family of POCOP Pincer Complexes with Nickel: Reactivity Towards CO₂ and Phenylacetylene. *Chem. - Eur. J.* **2014**, *20*, 11894–11902.
- Jonasson, K. J.; Mousa, A. H.; Wendt, O. F. Synthesis and characterisation of POC_{sp}₃OP supported Ni(II) hydroxo, hydroxycarbonyl and carbonate complexes. *Polyhedron* **2018**, *143*, 132–137.

- (24) van de Kuil, L. A.; Grove, D. M.; Gossage, R. A.; Zwikker, J. W.; Jenneskens, L. W.; Drenth, W.; van Koten, G. Mechanistic Aspects of the Kharasch Addition Reaction Catalyzed by Organonickel(II) Complexes Containing the Monoanionic Terdentate Aryldiamine Ligand System $[C_6H_2(CH_2NMe_2)_2-2,6-R-4]$. *Organometallics* **1997**, *16*, 4985–4994.
- (25) Cámpora, J.; Palma, P.; del Río, D.; Álvarez, E. CO Insertion Reactions into the M–OH Bonds of Monomeric Nickel and Palladium Hydroxides. Reversible Decarbonylation of a Hydroxycarbonyl Palladium Complex. *Organometallics* **2004**, *23*, 1652–1655.
- (26) Schmeier, T. J.; Hazari, N.; Incarvito, C. D.; Raskatov, J. A. Exploring the reactions of CO₂ with PCP supported nickel complexes. *Chem. Commun.* **2011**, *47*, 1824–1826.
- (27) Schmeier, T. J.; Nova, A.; Hazari, N.; Maseras, F. Synthesis of PCP-supported nickel complexes and their reactivity with carbon dioxide. *Chem. - Eur. J.* **2012**, *18*, 6915–6927.
- (28) Liang, L.-C.; Lin, J.-M.; Hung, C.-H. Nickel(II) Complexes of Bis(2-diphenylphosphinophenyl)amide. *Organometallics* **2003**, *22*, 3007–3009.
- (29) Liang, L.-C.; Chien, P.-S.; Lin, J.-M.; Huang, M.-H.; Huang, Y.-L.; Liao, J.-H. Amido Pincer Complexes of Nickel(II): Synthesis, Structure, and Reactivity. *Organometallics* **2006**, *25*, 1399–1411.
- (30) Chakraborty, S.; Krause, J. A.; Guan, H. Hydrosilylation of Aldehydes and Ketones Catalyzed by Nickel PCP-Pincer Hydride Complexes. *Organometallics* **2009**, *28*, 582–586.
- (31) Liang, L.-C.; Chien, P.-S.; Lee, P.-Y. Phosphorus and Olefin Substituent Effects on the Insertion Chemistry of Nickel(II) Hydride Complexes Containing Amido Diphosphine Ligands. *Organometallics* **2008**, *27*, 3082–3093.
- (32) Castonguay, A.; Spasyuk, D. M.; Madern, N.; Beauchamp, A. L.; Zargarian, D. Regioselective Hydroamination of Acrylonitrile Catalyzed by Cationic Pincer Complexes of Nickel(II). *Organometallics* **2009**, *28*, 2134–2141.
- (33) Lefèvre, X.; Spasyuk, D. M.; Zargarian, D. New POCOP-type pincer complexes of Nickel(II). *J. Organomet. Chem.* **2011**, *696*, 864–870.
- (34) Vabre, B.; Lambert, M. L.; Petit, A.; Ess, D. H.; Zargarian, D. Nickelation of PCP- and POCOP-Type Pincer Ligands: Kinetics and Mechanism. *Organometallics* **2012**, *31*, 6041–6053.
- (35) Gutsulyak, D. V.; Piers, W. E.; Borau-Garcia, J.; Parvez, M. Activation of Water, Ammonia, and Other Small Molecules by PCarbeneP Nickel Pincer Complexes. *J. Am. Chem. Soc.* **2013**, *135*, 11776–11779.
- (36) Vabre, B.; Petiot, P.; Declercq, R.; Zargarian, D. Fluoro and Trifluoromethyl Derivatives of POCOP-Type Pincer Complexes of Nickel: Preparation and Reactivities in S_N2 Fluorination and Direct Benzoylation of Unactivated Arenes. *Organometallics* **2014**, *33*, 5173–5184.
- (37) Borau-Garcia, J.; Gutsulyak, D. V.; Burford, R. J.; Piers, W. E. Selective hydration of nitriles to amides catalysed by PCP pincer supported nickel(ii) complexes. *Dalton transactions* **2015**, *44*, 12082–12085.
- (38) Shih, W.-C.; Ozerov, O. V. One-Pot Synthesis of 1,3-Bis(phosphinomethyl)arene PCP/PNP Pincer Ligands and Their Nickel Complexes. *Organometallics* **2015**, *34*, 4591–4597.
- (39) LaPierre, E. A.; Piers, W. E.; Spasyuk, D. M.; Bi, D. W. Activation of Si-H bonds across the nickel carbene bond in electron rich nickel PCarbeneP pincer complexes. *Chem. Commun.* **2016**, *52*, 1361–1364.
- (40) Spasyuk, D. M.; Zargarian, D.; van der Est, A. New POCN-Type Pincer Complexes of Nickel(II) and Nickel(III). *Organometallics* **2009**, *28*, 6531–6540.
- (41) Spasyuk, D. M.; Zargarian, D. Monomeric and dimeric nickel complexes derived from a pincer ligand featuring a secondary amine donor moiety. *Inorg. Chem.* **2010**, *49*, 6203–6213.
- (42) Mougang-Soumé, B.; Belanger-Gariépy, F.; Zargarian, D. Synthesis, Characterization, and Oxidation of New POCNimine-Type Pincer Complexes of Nickel. *Organometallics* **2014**, *33*, 5990–6002.
- (43) Smith, J. B.; Miller, A. J. M. Connecting Neutral and Cationic Pathways in Nickel-Catalyzed Insertion of Benzaldehyde into a C–H Bond of Acetonitrile. *Organometallics* **2015**, *34*, 4669–4677.
- (44) Smith, J. B.; Kerr, S. H.; White, P. S.; Miller, A. J. M. Thermodynamic Studies of Cation–Macrocyclic Interactions in Nickel Pincer–Crown Ether Complexes Enable Switchable Ligation. *Organometallics* **2017**, *36*, 3094–3103.
- (45) Fleckhaus, A.; Mousa, A. H.; Lawal, N. S.; Kazemifar, N. K.; Wendt, O. F. Aromatic PCN Palladium Pincer Complexes. Probing the Hemilability through Reactions with Nucleophiles. *Organometallics* **2015**, *34*, 1627–1634.
- (46) Mousa, A. H.; Fleckhaus, A.; Kondrashov, M.; Wendt, O. F. Aromatic PCN pincer palladium complexes: forming and breaking CC bonds. *J. Organomet. Chem.* **2017**, *845*, 157–164.
- (47) Burger, B. J.; Bercaw, J. E. In *New Developments in the Synthesis, Manipulation and Characterization of Organometallic Compounds*; Wayda, A.; Darensbourg, M. Y., Eds.; American Chemical Society: Washington, DC, 1987; Vol. 357.
- (48) *Crysalis CCD*; Oxford Diffraction Ltd.: Abingdon, U.K., 2005.
- (49) *Crysalis RED*; Oxford Diffraction Ltd.: Abingdon, U.K., 2005.
- (50) Sheldrick, G. M. SHELXT - Integrated space-group and crystal-structure determination. *Acta Crystallogr., Sect. A: Found. Adv.* **2015**, *71*, 3–8.
- (51) Sheldrick, G. M. Crystal structure refinement with SHELXL. *Acta Crystallogr., Sect. C: Struct. Chem.* **2015**, *71*, 3–8.
- (52) Dolomanov, O. V.; Bourhis, L. J.; Gildea, R. J.; Howard, J. A. K.; Puschmann, H. *J. Appl. Crystallogr.* **2009**, *42*, 339–341.
- (53) *CrystalMaker*, version 8.7; CrystalMaker Software; Oxfordshire, U.K., 2010.
- (54) Martínez-Prieto, L. M.; Melero, C.; del Río, D.; Palma, P.; Cámpora, J.; Álvarez, E. Synthesis and Reactivity of Nickel and Palladium Fluoride Complexes with PCP Pincer Ligands. NMR-Based Assessment of Electron-Donating Properties of Fluoride and Other Monoanionic Ligands. *Organometallics* **2012**, *31*, 1425–1438.
- (55) Wieghardt, K.; Walz, W.; Nuber, B.; Weiss, J.; Ozarowski, A.; Stratemeier, H.; Reinen, D. Crystal structure of bis[bis(1,4,7-triazacyclononane)nickel(III)] dithionate heptahydrate and its single-crystal EPR spectrum. *Inorg. Chem.* **1986**, *25*, 1650–1654.
- (56) Wang, Y. L.; Beach, M. W.; Pappenhagen, T. L.; Margerum, D. W. Mixed-ligand complexes of tetracyanonickelate(III) and dynamic Jahn-Teller distortions of hexacyanonickelate(III). *Inorg. Chem.* **1988**, *27*, 4464–4472.
- (57) Yoo, C.; Kim, J.; Lee, Y. Synthesis and Reactivity of Nickel(II) Hydroxycarbonyl Species, NiCOOH-κC. *Organometallics* **2013**, *32*, 7195–7203.
- (58) Cámpora, J.; Palma, P.; del Río, D.; Conejo, M. M.; Álvarez, E. Synthesis and Reactivity of a Mononuclear Parent Amido Nickel Complex. Structures of Ni[C₆H₃-2,6-(CH₂PⁱPr₂)](NH₂) and Ni[C₆H₃-2,6-(CH₂PⁱPr₂)](OMe). *Organometallics* **2004**, *23*, 5653–5655.
- (59) Johansson, R.; Öhrström, L.; Wendt, O. F. Hydrogen Bond Control of Dimensionality in Organometallic {2,6-Bis[(di-*t*-butylphosphino)methyl]phenyl}palladium(II) Compounds: Dimers, Chains, and a 3D-Net with an Apparent Channel Structure. *Cryst. Growth Des.* **2007**, *7*, 1974–1979.
- (60) Johansson, R.; Wendt, O. F. Synthesis and Reactivity of (PCP) Palladium Hydroxy Carbonyl and Related Complexes toward CO₂ and Phenylacetylene. *Organometallics* **2007**, *26*, 2426–2430.
- (61) Fulmer, G. R.; Miller, A. J. M.; Sherden, N. H.; Gottlieb, H. E.; Nudelman, A.; Stoltz, B. M.; Bercaw, J. E.; Goldberg, K. I. NMR Chemical Shifts of Trace Impurities: Common Laboratory Solvents, Organics, and Gases in Deuterated Solvents Relevant to the Organometallic Chemist. *Organometallics* **2010**, *29*, 2176–2179.
- (62) Boro, B. J.; Duesler, E. N.; Goldberg, K. I.; Kemp, R. A. Synthesis, Characterization, and Reactivity of Nickel Hydride Complexes Containing 2,6-C₆H₃(CH₂PR₂)₂ (R = *t*Bu, *c*Hex, and *i*Pr) Pincer Ligands. *Inorg. Chem.* **2009**, *48*, 5081–5087.

(63) Breitenfeld, J.; Scopelliti, R.; Hu, X. Synthesis, Reactivity, and Catalytic Application of a Nickel Pincer Hydride Complex. *Organometallics* **2012**, *31*, 2128–2136.